Cytometry
PART A
Journal of the
International Society for
Advancement of Cytometry

Quantitation of Yeast Cell–Cell Fusion Using Multicolor Flow Cytometry

Valentina Salzman,[1*] Valentina Porro,[2] Mariela Bollati-Fogolín,[2] Pablo S. Aguilar[1,3*]

[1]Laboratorio De Biología Celular De Membranas, Institut Pasteur De Montevideo, Montevideo 11400, Uruguay

[2]Cell Biology Unit, Institut Pasteur De Montevideo, Montevideo 11400, Uruguay

[3]Laboratorio de Biología Celular de Membranas, Instituto De Investigaciones Biotecnológicas, Universidad Nacional De San Martín, CONICET, San Martín, Buenos Aires, Argentina

Correspondence to: Pablo S. Aguilar, Laboratorio de Biología Celular de Membranas, Institut Pasteur de Montevideo, Mataojo 2020, Montevideo 11400, Uruguay. E-mail: pablo.aguilar@pasteur.edu.uy. Valentina Salzman, Laboratorio de Biología Celular de Membranas, Instituto de Investigaciones Biotecnológicas, Universidad Nacional de San Martín, CONICET, San Martín, Buenos Aires, Argentina. E-mail: vsalzman@iib.unsam.edu.ar

ISAC
International Society for Advancement of Cytometry

● **Abstract**
Mating of haploid *Saccharomyces cerevisiae* cells of opposite sex provides a powerful model system to study the cell–cell fusion. However, a rapid and standardized method is much needed for quantitative assessment of fusion efficiency. The gold standard method relies on counting mating pairs in fluorescence microscopy images. This current method is limited by expectancy bias and it is time consuming, restricting the number of both cell–cell fusion events and strains that can be analyzed at once. Automatic approaches present a solution to these limitations. Here, we describe a novel flow cytometric approach that is able to quickly both identify mating pairs within a mixture of gametes and quantify cell fusion efficiency. This method is based on staining the cell wall of yeast populations with different Concanavalin A–fluorophore conjugates. The mating subpopulation is identified as the two-colored events set and fused and unfused mating pairs are subsequently discriminated by green fluorescent protein bimolecular complementation. A series of experiments was conducted to validate a simple and reliable protocol. Mating efficiency in each sample was determined by flow cytometry and compared with the one obtained with the current gold standard technique. The results show that mating pair counts using both methods produce indistinguishable outcomes and that the flow cytometry-based method provides quantitative relevant information in a short time, making possible to quickly analyze many different cell populations. In conclusion, our data show multicolor flow cytometry-based fusion quantitation to be a fast, robust, and reliable method to quantify the cell–cell fusion in yeast. © 2015 International Society for Advancement of Cytometry

● **Key terms**
fertilization; mating; bi-molecular complementation; *Saccharomyces cerevisiae*; flow cytometry; microscopy

ALL eukaryotic organisms feature essential cellular processes that require membrane fusion to proceed. Cell–cell fusion underlies many developmental processes such as fertilization (1,2), the fusion of myocytes to produce skeletal muscle fibers (3–5), trophoblast fusion (6) during placenta development, and the fusion of macrophage/monocyte-derived cells to produce osteoclasts for bone remodeling and multinucleated giant cells to scavenge large foreign bodies (7,8). Although it is highly debated, cell–cell fusion has also been implicated in the regeneration of tissues after injury (9) and carcinogenesis (10,11).

Biological membranes do not fuse spontaneously; rather, specialized proteins, called fusogens, which are necessary and sufficient to fuse cell membranes, catalyze fusion. Many fusogens that mediate the entry of enveloped viruses have been identified (12–14), as well as the group of SNAREs proteins, the minimal machinery that promotes intracellular vesicular fusion (15,16). In remarkable contrast to viral and intracellular vesicular membrane fusion, the proteins that catalyze cell–cell fusion had remained elusive for years. Recent study has led to the discovery of two families of fusogens that mediate cell–cell fusion. One family mediates placenta development in different mammals (6,17–19) and the other mediates epithelial tissue development

in *Caenorhabditis elegans* (Syncytins and F proteins, respectively) (12,20,21). As mechanisms and fusogens for most cell–cell fusion events are still unknown, many research groups aim to identify new cellular fusogens and to determine the mechanistic basis of this highly conserved cellular process. A prevailing view suggests that the molecular machineries that catalyze cell–cell fusion may have evolved independently, and thus differ from one biological system to another (22,23). Different model systems, therefore, are invaluable to identify shared principles that may reside at the core of the cell–cell fusion reaction.

Fusion of haploid yeast cells of opposite mating types provides a powerful model system to study the cell–cell fusion (24). *Saccharomyces cerevisiae* haploid cells behave as gametes existing as one of the two mating types, **a** or α, which secrete a sexual pheromone (**a** factor or α factor, respectively) that is sensed by the complementary mating type. Upon pheromone detection, a signaling cascade is activated leading to cell-cycle arrest, transcriptional reprogramming, and polarized growth toward the site with highest pheromone concentration, that is, toward the mating partner (25). Once in contact, the cell walls of the mating partners adhere forming a mating pair. Cell-wall material located at the cell–cell interface is then precisely removed, allowing the plasma membranes to oppose and fuse forming a dinucleate zygote with a common cytoplasm. Then, both nuclei are drawn toward each other and undergo karyogamy giving rise to an **a**/α diploid cell (24).

During more than 30 years, yeast's powerful genetic approaches have lead to the identification of many players involved in every step of mating: from pheromone production and detection to karyogamy (for a review see Refs. 26,27)). Surprisingly, phenotypic analysis of the so-called cell–cell fusion mutants did not pinpointed any of the identified genes as a bona fide fusogen. *fus1* was the first cell–cell fusion mutant to be studied (28,29), Fus1p was initially thought to mediate either the cell-wall degradation or the plasma membrane fusion step but further characterization proposed that a more likely role for Fus1p is to promote fusion pore expansion (30). A bioinformatics approach identified pheromone-regulated multispanning membrane protein 1 (Prm1p) as a candidate protein involved in the bilayer fusion step *per se* (31). However, careful examination of *prm1Δ* x *prm1Δ* mating pairs suggests that Prm1p is not a fusogen but more likely a regulator of the cell–cell fusion machinery (31–34). Another plasma membrane protein, Fig1p, has also been identified having a Prm1p-like function in cell–cell fusion although its molecular role and functional relationship with Prm1p and Fus1p remains uncertain (35). The apparent failure of yeast classical genetic approaches in identifying bona fide fusogens suggests that these machineries might have one or more of the following properties. Yeast fusogens can be protein hetero-complexes and therefore be of multigenic nature. Another possibility is that there is more than one fusogenic gene per genome. Finally, fusogens can also act unilaterally, that is loss of function in both mating partners is needed to observe a phenotype. In any case, the current scenario presents still elusive machineries mediating cell–cell fusion during yeast mat-
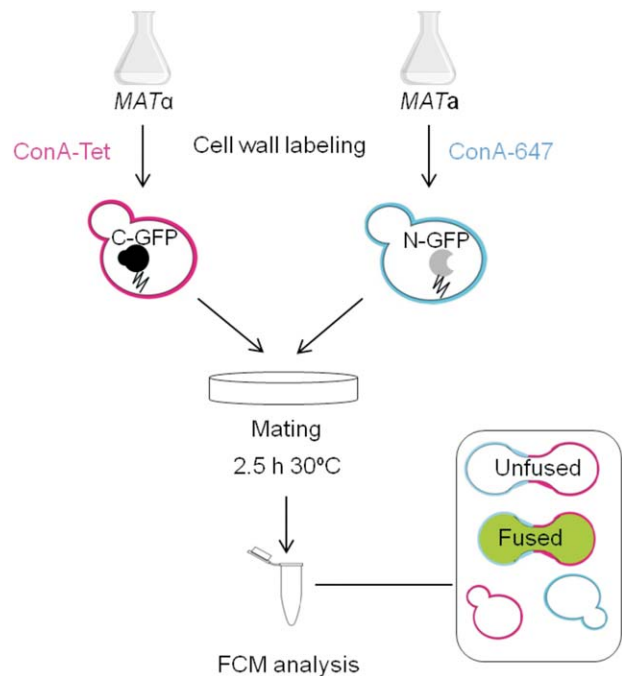
Figure 1. Experiment overview. *MAT*α and *MAT***a** *S. cerevisiae* strains are cultivated to exponential growth phase. Cells are separately stained with ConA–fluorophore conjugates (ConA-Tet or ConA-647). Each strain harbors a GFP fragment (N-GFP or C-GFP) fused to a dimerization domain (zig-zag tail), BiFC occurs when the cytoplasmatic contents of two cells of different mating type mix. Stained cells are mixed, concentrated, and incubated in a solid medium plate at 30°C. After 2.5 h, a "mating sample" is obtained containing fused mating pairs (ConA-Tet/ConA-647/GFP) and unfused mating pairs (ConA-Tet/ConA-647) among other possible combinations of stained and unstained cells (for details, see the text). By FCM analysis, different mating pair sub-populations are identified and yeast cell fusion efficiency is quantified. [Color figure can be viewed in the online issue, which is available at wileyonlinelibrary.com.]

ing and therefore biochemical and bioinformatics approaches may be helpful in finding these proteins. Given the possible functional redundancy of fusogenic actors within or between mating partners combinatorial analysis of candidate genes should be seriously considered.

In this context, high-throughput techniques for the analysis of cell fusion efficiency of multiple yeast strains are a key part of the yeast fusion machine discovery process. The current reference method used to score cell fusion efficiency is to observe mating reactions by microscopy. In this method, pairs are first morphologically identified in bright field (BF) microscopy images. Mating pairs are peanut shaped, with two lobes connected by a wide neck, whereas individual cells are oval shaped. To distinguish fused from unfused pairs, at least one partner expresses a soluble cytosolic fluorescent protein. Green fluorescent protein (GFP) is usually used as a marker for cytoplasmic mixing as it can rapidly diffuse through the fusion pore linking the plasma membranes of two cells. Subsequent analysis of whether the fluorescent protein has spread to both cells (indicating successful cell–cell fusion) or remained restricted to one mating partner (indicating a failure

to fuse) enables fusion efficiency quantitation (36). As analysis of at least 200 mating pairs is usually necessary to yield a statistically significant result, this is a very time-consuming method. To overcome this limitation, we developed and validate a flow cytometry (FCM)-based cell fusion assay which has been optimized to quickly quantify the fraction of fused pairs from the total number of mating pairs in complex mating samples. With this automatic approach, the analysis of cell fusion efficiency of multiple yeast strains is possible in relatively short time providing quantitative, accurate, and reproducible data and successfully detecting fusion defects.

MATERIALS AND METHODS

Experiment Overview

To quantify cell–cell fusion in yeast, haploid cells are harvested in exponential growth phase, stained, and then allowed to mate (Fig. 1). *MAT*a and *MAT*α strains are distinguished by staining each strain with different *Canavalia ensiformis'* Concanavalin A (ConA)–fluorophore conjugates and mating pairs are revealed as two-colored entities. Fused mating pairs are easily distinguished from unfused pairs by bimolecular fluorescence complementation (BiFC) as each strain synthesizes a nonfluorescent fragment of GFP protein that associates with each other forming a fluorescent complex when cell–cell fusion occurs (37).

Staining Reagents

ConA-Alexafluor 647 (ConA-647) (Catalog #C21421, 1 mg/mL stock solution in 0.1M sodium bicarbonate) and ConA-Tetramethylrhodamine (ConA-Tet) (Catalog #C860, 5 mg/mL stock solution in 0.1M sodium bicarbonate) were acquired from Life Technologies, Grand Island, NY. Stock solutions were aliquoted and stored at −20°C protected from light.

Media and Yeast Strains

Synthetic defined (SD) and complex yeast extract peptone (YP) media were prepared and supplemented with 2% of glucose. All *S. cerevisiae* strains (Supporting Information Table S1) used in this study are derived from BY4743. YM2901 is a *MAT*a strain containing the amino terminus of eGFP fused to a leucine zipper dimerization domain (37). YM2903 is a *MAT*α strain containing the carboxy terminus of eGFP fused to a leucine zipper dimerization domain as well as an mCherry marker driven by the promoter of the gene TEF2 (pTEF2) integrated at the *LYS1* locus (37). Gene replacements were generated with the polymerase chain reaction (PCR) transformation technique (38,39) and confirmed by PCR.

Flow Sample Preparation

Growth conditions. *MAT*α and *MAT*a *S. cerevisiae* strains cultivated to exponential growth phase were the starting point of flow sample preparation (Fig. 1). On the day preceding the multicolor FCM-based cell fusion assay, cultures of each cell type were inoculated and grown with shaking overnight at 25°C to mid-log phase (OD$_{600\,nm}$ = 0.3–0.4) in SD or YPD medium.

Cell wall staining of yeast cells. To stain haploid cells' surface with a ConA–fluorophore conjugate, 4 ODs of a mid-log

phase culture of each mating type were harvested by centrifuging 3 min at 3,000g in a swinging bucket rotor in 15 mL screw-cap centrifuge tubes. All steps were performed at room temperature (RT). Pellets were washed twice with 5 mL of D-phosphate-buffered saline (PBS) (Life technologies, Grand Island, NY, Catalog #14040–133) and resuspended in 1 mL of this buffer by vortexing. Then, 500 μL of *MAT*a and *MAT*α cell suspensions was taken apart and stained with ConA-647 or ConA-Tet, respectively, for 30 min in the dark. Working concentrations of ConA–fluorophore conjugates were optimized as described below. After the incubation step, stained and unstained cells were washed twice with 2.5 mL of YPD medium and resuspended in 1.5 mL of YPD. The indicated starting cell densities and volumes are adequate for the complete analysis of one mating cross.

Yeast mating conditions. After cell-wall staining step, equal numbers of cells (300 μL of the 1.5 mL YPD suspension, around 0.4 ODs) of each mating type were mixed in a total volume of 5 mL YPD and vacuumed to a 25-mm diameter, 0.45 μm-pore size nitrocellulose filter (Millipore, Billerica, MA; Catalog # HAWP02500). The filter was cell-side up on SD or YPD plates and then incubated for 2.5 h at 30°C. After this step, approximately 20% of the total cell population engaged in mating and went through the whole process of diploid cell formation giving enough mating pairs to analyze (see results below). Cells were finally scraped off the filter in 600 μL of ice-cold PBS buffer. We proceed similarly with haploid samples. The analysis of a mating cross includes three ConA-Tet *MAT*α × ConA-647 *MAT*a mating samples, an unstained haploid sample of each mating type, a ConA-Tet single-stained *MAT*α haploid sample, a ConA-647 single-stained *MAT*a haploid sample and a *MAT*α unstained × *MAT*a unstained mating sample. To quantify fusion efficiency of a mating cross, three independent experiments were done.

Instrument Details

Flow sample analysis was performed using a CyAn™ ADP LX, 7 color (Beckman Coulter, USA) flow cytometer equipped with two lasers (488 and 635 nm). Data acquisition and analysis were achieved using Summit v4.3 software (Dako Cytomation). Cytometer setup: the blue laser (488 nm) was selected to excite GFP and tetramethylrhodamine (Tet), whereas the red laser (633 nm) for the Alexa Fluor 647 and 530/40; 575/25 and 665/20 nm band pass filters were used for the photomultipliers (PMTs) collecting the GFP, Tet, and Alexa Fluor 647 signals, respectively. FSC and SSC peak signals were displayed on a linear scale and GFP, Tet, and Alexa Fluor 647 peak signals were amplified logarithmically. To achieve satisfactory flow rates, flow samples were diluted 1:10 with PBS and transferred to appropriate FCM analysis tubes. It is important to vortex briefly 5 s just before mounting the tube in the cytometer to ensure a homogeneous cell suspension.

Data Analysis

Debris removal. The gating strategy comprised a FSC versus SSC cell region that excludes cellular debris and irrelevant small particles (Fig. 2A, gate R1). This region was applied to
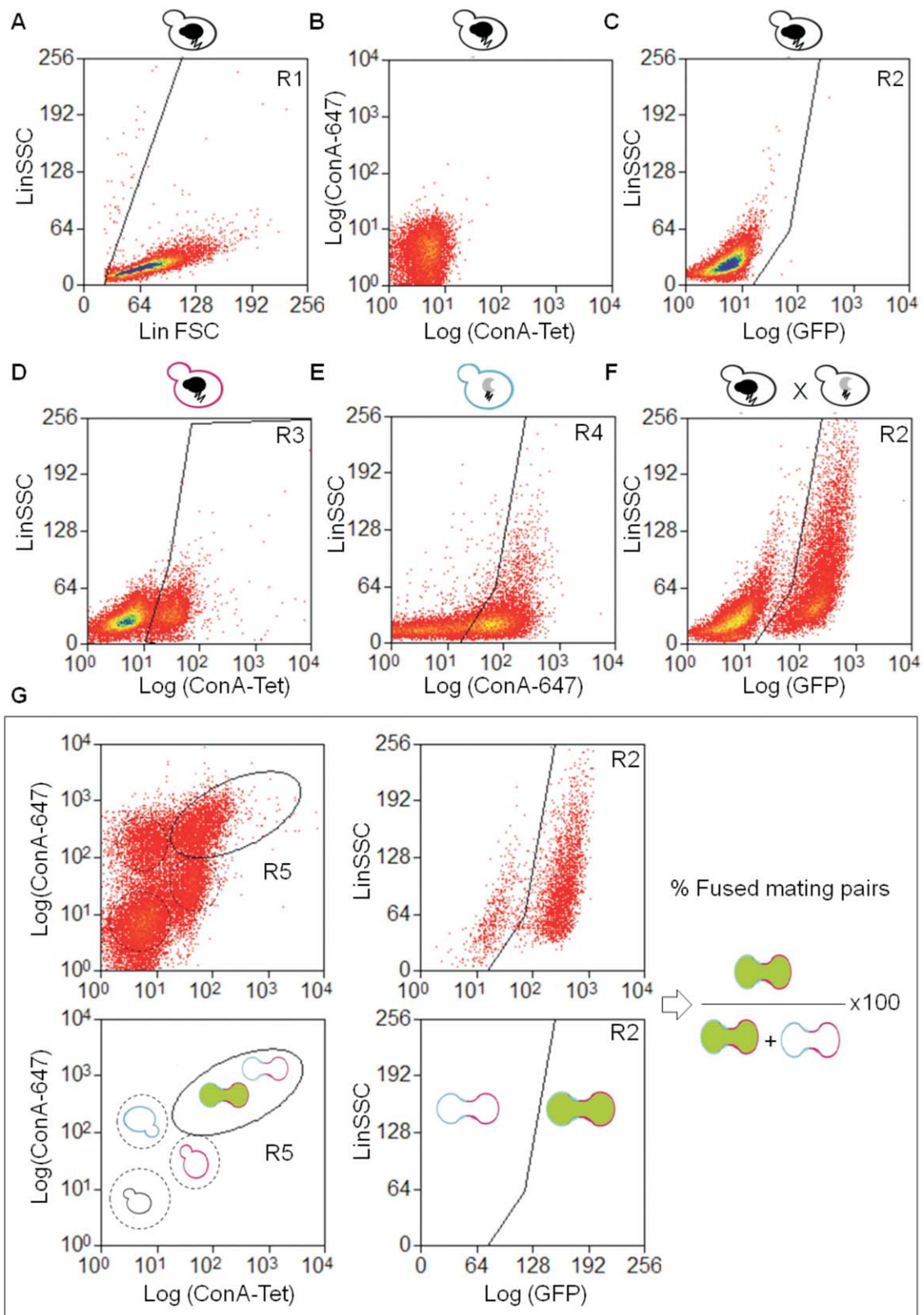
Figure 2. Gate strategy. **A**: Debris removal. R1 gate is defined in a SSC versus FSC dot plot to eliminate cellular debris; R1 is then applied to all subsequent plots. **B, C**: Unstained controls. A haploid cells unstained sample is used to set voltages and gains in ConA-Tet versus ConA-647 and SSC versus GFP plots. GFP⁻/GFP⁺ boundary is set. **D–F**: Single-stained compensation controls. *MAT*α ConA-Tet single-stained haploid cells, *MAT***a** ConA-647 single-stained haploid cells, and a fusion mix sample obtained from a *MAT*α unstained × *MAT***a** unstained mating are used as single-colored compensation controls. R3 and R4 gates contain *MAT*α ConA-Tet⁺ and *MAT***a** ConA-647⁺ populations, respectively. R2 GFP⁺ cells comprise fused mating pairs and diploid daughter cells. All controls are vacuumed filtered and incubated 2.5 h at 30°C before FCM. **G**: Cell fusion quantitation. A mating sample obtained from *MAT*α ConA-Tet × *MAT***a** ConA-647 cross is analyzed in a ConA-Tet versus ConA-647 dot plot where two-colored events are selected (R5). Entities present in each subpopulation are schematized. The R5 gate containing mating pair subpopulation is then applied to a SSC versus GFP plot to differentiate between fused (R2) and unfused pairs. A typical wt × wt cross is shown (YM2901 × YM2903, Supporting Information Table S1). The percentage of fused mating pairs is calculated from SSC versus GFP plot as the number of fused pairs over total number of events in this plot × 100. [Color figure can be viewed in the online issue which is available at wileyonlinelibrary.com]

all subsequent plots so that only gated events were displayed. The trigger channel was the FSC and the threshold value was set up such that debris and undesired events should be eliminated without inadvertently eliminating relevant events. For accurate statistical analyses, 30,000 gated events on an FSC versus SSC dot plot per sample were collected.

Controls and compensation settings. Unstained cells and mating pairs were used as negative controls. Using an unstained *MATα* sample, voltage settings and amplifiers gains were set so that negative values lie in the first log scale of ConA-647 and ConA-Tet axes in a ConA-647 versus ConA-Tet dot plot (Fig. 2B). In a similar way, the voltage and gain were adjusted in a SSC versus GFP dot plot using the unstained *MATα* sample (Fig. 2C). A gate was defined to distinguish GFP negative (GFP$^-$) from GFP positive (GFP$^+$, named as R2) populations (Fig. 2C). The samples containing the complete range of signals (positive and negative) were used for further adjustment of voltage settings. For this purpose, a ConA-Tet single-stained MATα haploid sample (Fig. 2D), a ConA-647 MATa single-stained haploid sample (Fig. 2E) and a mating cross of unstained cells as GFP single-colored control (Fig. 2F) were included in the experiment. As single-stained samples were treated in the same manner as mating samples, daughter cells emerge after staining during standard mating conditions (2.5 h at 30°C), resulting in the accumulation of a fraction of cells with unstained cell walls. Therefore, not only positive but also negative events were detected in these samples. Instrument settings were saved and used unchanged for all experiments to allow direct comparison between them. Spectral overlap between fluorophores was compensated using the single-stained samples as compensation controls and off-line compensation. For correct compensation, the median of the negative population was set equally to the median of the positive population in the spillover channel. As cell-wall staining may vary between experiments, and thus affecting the compensation values, compensation controls were included in every experiment.

Cell fusion quantitation. After acquiring the controls, stained mating samples were analyzed to quantify cell fusion efficiency. First, mating pairs were identified as double-stained entities in a ConA-Tet versus ConA-647 dot plot (ConA-Tet positive [ConA-Tet$^+$]/ConA-647 positive [ConA-647$^+$] subpopulation, R5 gate, Fig. 2G, left panels). The defined R5 gate was then applied to a SSC versus GFP dot plot (Fig. 2G, right panels). The percentage of fused mating pairs was calculated as the number of fused mating pairs (GFP$^+$) over total number of events in this plot × 100 (Fig. 2G). Mating crosses were performed by triplicate in each standard experiment and the percentage of fused mating pairs was calculated as the average of the three obtained values.

Cell-Wall Staining Optimization

Before cell-wall staining, the optimal concentration of reagents should be optimized for each set of reagents and flow cytometer. To determine the appropriate amounts of ConA–

fluorophore conjugates, *MATα* and *MATa* strains were stained with incremental concentrations of ConA-Tet or ConA-647, respectively. To this end, 6 × 0.4 ODs of log-phase cultures of each mating type were harvested in 15 mL of screw-cap centrifuge tubes by centrifuging 3 min at 3,000g in a swinging bucket rotor. Pellets were washed twice with 3 mL of D-PBS and resuspended in 600 μL of this buffer. Then, 100 μL of aliquots of cells was stained for 30 min in the dark and the final concentrations of ConA–fluorophore conjugates ranged between 0 and 500 μg/mL. After the incubation step, cells were washed twice with 0.5 mL of YPD medium to remove excess of dye. All steps were performed at RT. Then, each sample was resuspended in a total volume of 5 mL of YPD and vacuumed to a 0.45-μm-pore size nitrocellulose filter (Millipore, Billerica, MA; Catalog # HAWP02500). Each filter was cell-side up on SD plates which were incubated for 2.5 h at 30°C. Cells were finally scraped off the filter in 600 μL of ice-cold PBS buffer and then subjected to analysis by FCM. For data analysis, a region was defined in the FSC versus SSC dot plot, excluding cellular debris as shown in Figure 2A. The fluorescence from *MATα* ConA-Tet- and *MATa* ConA-647-stained cells was represented in ConA-Tet and ConA-647 histograms, respectively. For each condition, the stain index (Si) was calculated. The Si is defined as the difference (*D*) between positive and background peak medians divided by the spread of the background peak *W* (calculated as two times the standard deviation [SD] of the negative population). Si = *D*/ *W* = (median positive peak − median negative peak)/2 × SD negative peak. The impact of cell-wall staining on cell viability was addressed. For this, ConA-647-stained and unstained samples were incubated with 1 μg/mL of propidium iodide (PI), which is excluded from viable cells. Fluorescence microscopy quantification of PI-positive cells showed no differences between samples, indicating that ConA–fluorophore conjugate staining does not affect cell viability (data not shown).

Fluorescence Microscopy

The samples analyzed by FCM were also examined by confocal fluorescence microscopy (Leica TCS-SP5) using a HCX PL APO 63×/NA1.40 CS oil objective. Sequential setting no. 1: 22% 633 nm laser power, PMT 2 (642–712 nm): gain 903, offset: 0. Sequential setting no. 2: 30% 514 nm laser power, PMT 1 (548–617 nm): gain 943, offset: 0; transmission PMT: gain 409, offset: 5. Sequential setting no. 3: 64% 488 nm laser power, PMT 1 (495–546 nm): gain 750, offset: −1. Pinhole: 191.0 μm. Zoom factor, 64%. Image analysis was performed using ImageJ (http://rsb.info.nih.gov/ij/).

Statistics

Data were expressed as the average ± SD of triplicates and three independent experiments were executed. Statistic calculations were performed using Prism Software version 5 (GraphPad) and StatGraphics Software version XVI. A *t*-test was used to test for differences in cell fusion efficiency between different sample treatments. Levene test was used to test for homogeneity of variances for cell fusion efficiency determinations of wild-type and mutant strains mating crosses by FCM and fluorescence microscopy. A two-way

ANOVA was used to test for significant differences in the determination of cell fusion efficiency between these groups. Bonferroni test was used for post hoc testing of differences between strains analyzed by FCM and fluorescence microscopy.

RESULTS

Cell-Wall Staining Optimization

In this study, a multicolor FCM-based assay to quantify cell–cell fusion in yeast was developed. The procedure is based on identifying different cell populations by staining the yeast cell wall with ConA conjugated to different fluorescent markers (40). The performance of the FCM setup must first be addressed to determine the optimal ConA–fluorophore conjugates concentration ranges. Although over staining often makes compensation between detecting channels very difficult to achieve or even can affect the biological process to be evaluated, under staining limits the number of events that can be resolved. To identify the appropriate concentration range for each ConA–fluorophore conjugate, haploid cells were stained, incubated at standard mating conditions (30°C for 2.5 h in SD plates) and analyzed by FCM (Fig. 3). When comparing Si values for the different ConA-647 staining conditions (Supporting Information Table S2), we found that resolution increased with ConA-647 concentration. However, as shown in Figure 3A, the unstained subpopulation fluorescence signal also became higher as the reagent concentration increased. Taking this into account, 20 μg/mL ConA-647 was selected as the final staining concentration as it is high enough to distinguish between ConA-647 positive and negative cells subpopulations while minimizing nonspecific fluorescence of the unstained subpopulation. It must be taken into account that the smaller concentration value that fulfilled this criterion was selected to minimize the reagent costs. When titrating ConA-Tet reagent (Fig. 3B), we found that the calculated Si values for each staining condition indicated that the maximum resolution was achieved with final concentrations $\geq$250 μg/ml of ConA-Tet (Supporting Information Table S2). Even doubling the fluorophore concentration did not correlate with an increase in the Si, and therefore 250 μg/mL of ConA-Tet was selected as the optimal concentration. It must be taken into account that if a flow cytometer equipped with a laser closer to ConA-Tet maximum excitation wavelength ($\sim$555 nm) is available (e.g., with a yellow–green laser), the final working concentration is expected to be smaller than the one used in this study.

Validation of ConA–Fluorophore Staining as a Permanent Label for Cell Fusion Quantitation

To use the surface staining as a permanent label for the quantitation of yeast cell fusion, staining conditions were developed to meet the following requirements: (1) the ConA–fluorophore label should be retained by the cells' surface under the standard mating conditions and (2) the staining procedure should not perturb cell fusion efficiency. To test whether the first criteria was fulfilled, haploid single-stained samples were obtained using optimized ConA–fluorophore

conjugates concentrations, vacuum-filtered and incubated for 0.5 or 2.5 h in SD agar plates at 30°C. By comparing the median ConA-Tet fluorescence intensity of the ConA-Tet$^+$ subpopulations, we determined that the older cell-wall components (i.e., mother cells' walls) retained more than 65% of the initial fluorescent label after the mating incubation period (Supporting Information Fig. S1A), similar median values of ConA-Tet$^+$ subpopulations were observed in cell fusion experiments (data not shown). In contrast, the newly synthesized cell wall of daughter cells was not stained (Supporting Information Fig. S1B) as previously reported (41,42). Similar results were found for ConA-647$^+$ subpopulations (data not shown). To test whether the second criterion was fulfilled, cell fusion efficiency of matings between $MAT\alpha$- and $MAT\mathbf{a}$-stained cells was analyzed by fluorescence microscopy. When cell fusion efficiency values derived from ConA–fluorophore-stained and unstained samples were compared, we found that they did not differ significantly (t-test, $P = 0.49$), indicating that the staining procedure causes minor or no perturbations to cell–cell fusion during mating of $S.$ $cerevisiae$ haploid cells (Fig. 4).

Mating Pairs Subpopulation Identification

Mating samples are complex cellular populations that include not only ConA–fluorophore-stained haploid cells and mating pairs but also unstained haploid cells (mostly daughter cells which were born during the mating incubation period), mating pairs where none or only one cell is stained and GFP$^+$ $\mathbf{a}/\alpha$ diploid daughter cells. Therefore, within a mating mixture ConA–fluorophore-double-stained entities can either be bona fide mating pairs, doublets (or higher order aggregates) formed by stochastic association of $MAT\mathbf{a}$ and $MAT\alpha$ cells or a mixture of both. To control whether the mating pair subpopulation was being properly gated in the ConA-647 versus ConA-Tet plots, a cell fusion assay between two sterile mutants, $MAT\mathbf{a}$ $ste2\Delta$ and $MAT\alpha$ $ste3\Delta$ was performed under standard conditions. As the $STE2$ and $STE3$ genes that codify for pheromones receptors had been deleted in these strains, these cells were not able to engage in the pheromone response pathway and therefore were not capable to form mating pairs (43,44). Accordingly, only a few events ConA-Tet$^+$/ConA-647$^+$ were detected in the mating pairs gate R5 (around 0.5% of total analyzed events, Fig. 5B). These events, which were GFP$^-$ (Fig. 5C), more likely consist of $MAT\mathbf{a}$/$MAT\alpha$ doublets or higher order aggregates formed by stochastic collision and unspecific cell tethering. A very effective way to dissociate nonspecifically tethered cells is to sonicate samples immediately before proceeding to FCM. As expected, when the same samples were treated (10 s at 10% amplitude with a microtip sonicator on ice) just before FCM data recording, <0.05% of total analyzed events were ConA-Tet$^+$/ConA-647$^+$ (Fig. 5E). Thus, we conclude that, under our mating conditions, approximately 0.5% of the total cell populations are false mating pairs formed by unspecific tethering of cells that, more likely, are not mating engaged.

As in a typical wt × wt mating mixture 22% of events are two colored, it can be assumed that nonspecific cell doublets
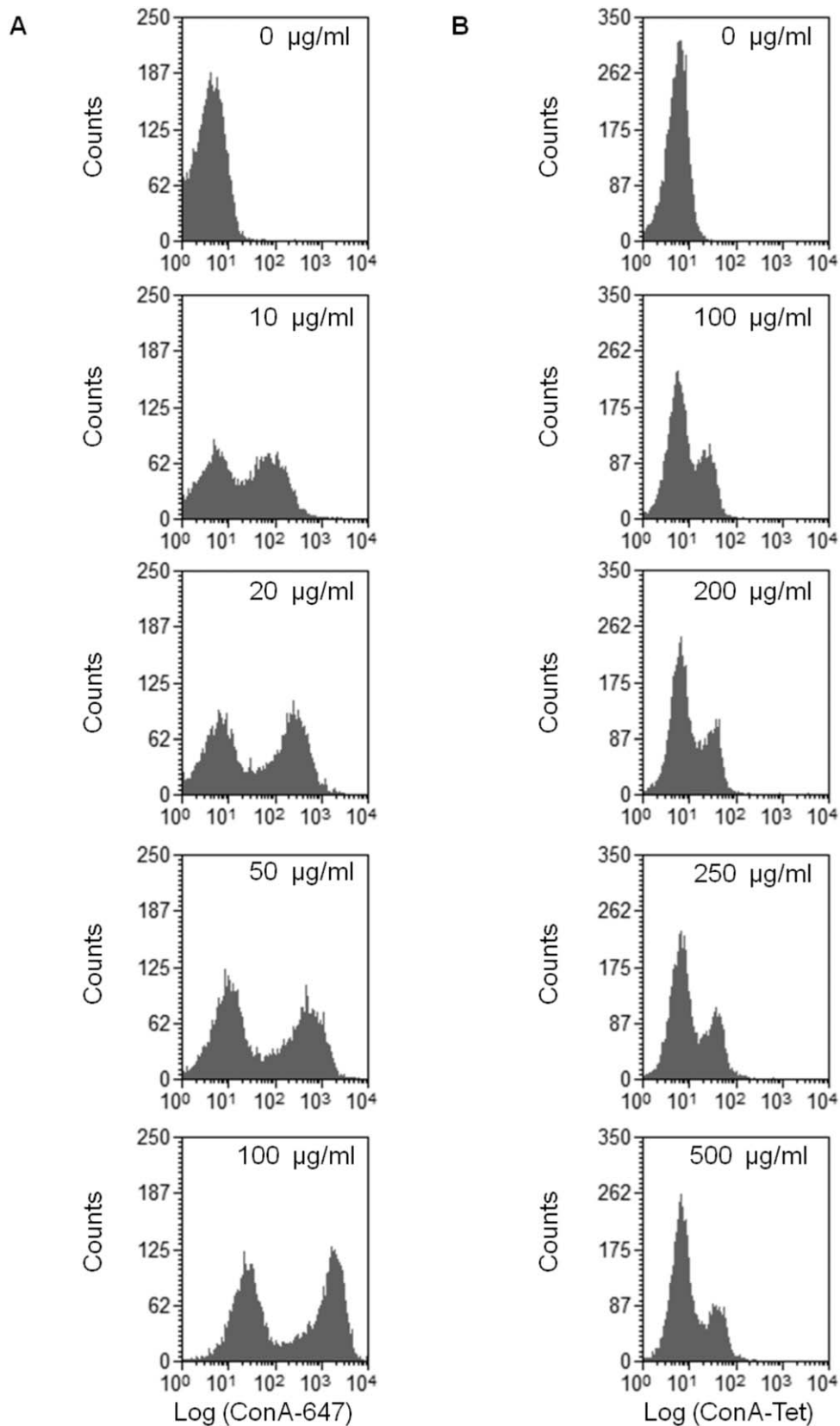
Figure 3. Cell-wall labeling optimization. **A**: *MAT*a cells (YM2901) were stained with 0, 10, 20, 50, or 100 μg/mL final concentration of ConA-647 for 30 min. **B**: *MAT*α cells (YM2903) were stained with 0, 100, 200, 250, or 500 μg/mL of final concentration of ConA-Tet for 30 min. Stained cells were vacuumed filtered and incubated 2.5 h at 30°C and analyzed by FCM. In total, 10,000 events were analyzed per sample.
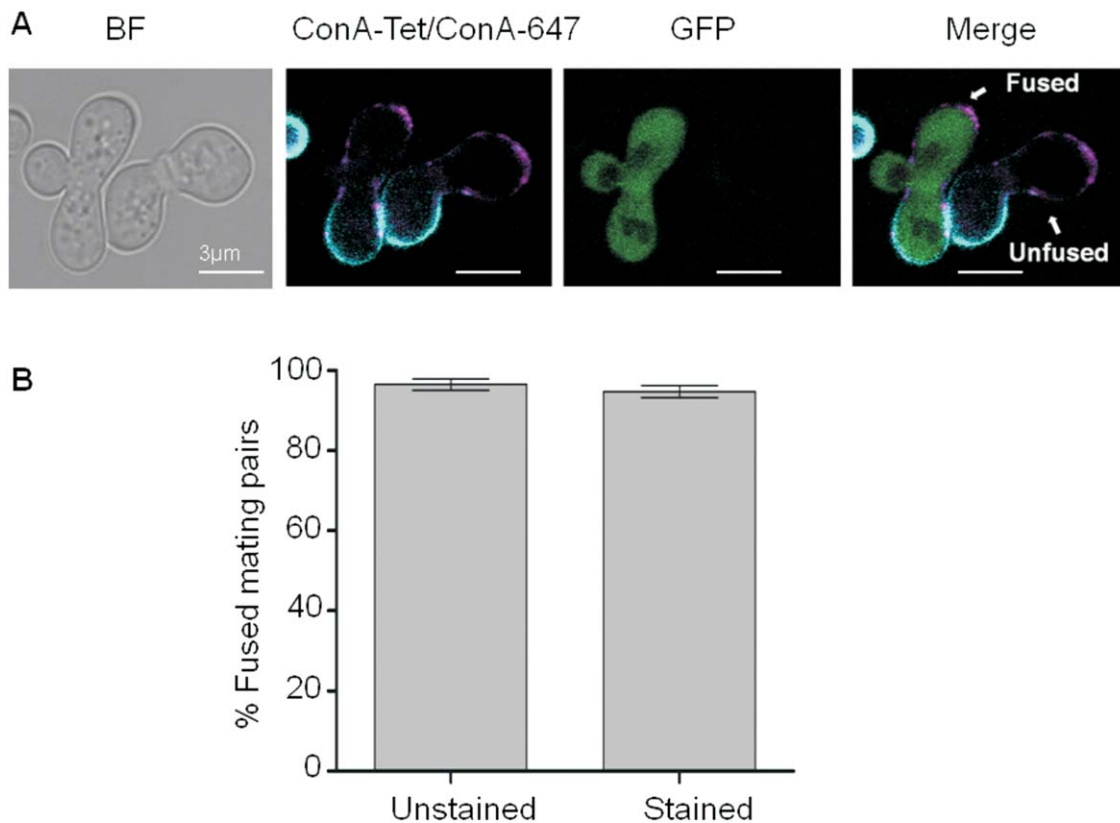
Figure 4. Staining procedure does not affect cell fusion efficiency. **A**: Quantitative cell fusion assays of wt × wt matings of stained or unstained cells were performed and then imaged and quantified by fluorescence microscopy. In ConA–fluorophore-stained cell mating samples, ConA-Tet$^+$/ConA-647$^+$ mating pairs were first identified by the presence of both ConA–fluorophore conjugates and then classified as fused (GFP$^+$) or unfused (GFP$^-$). In unstained samples, mating pairs were first morphologically identified in BF images and then classified as fused (GFP$^+$) or unfused (GFP$^-$). **B**: Bars indicate mean ± SD for three independent experiments with 200 mating pairs scored for each case. [Color figure can be viewed in the online issue which is available at wileyonlinelibrary.com]

represent approximately 2.3% of the two-colored mating pair population. Given that this false mating pair population is always GFP$^-$, we can assume that our FCM assay overestimates the unfused mating pair population in at least 2.3%. This value is smaller than the calculated interexperimental error among three independent cell fusion assays (relative standard error [RSE] = 5.3%; Supporting Information Table S3). In addition, no significant variation in cell fusion efficiency values was detected when a sonication step was included in the protocol (Supporting Information Fig. S2) (t-student, $P = 0.1$). In view of the obtained results, sample sonication before proceeding to FCM is avoided in the standard assay simplifying manipulation and reducing the time required for sample preparation.

Fused and Unfused Mating Pair Discrimination

Fused and unfused mating pair subpopulations are discriminated in a SSC versus GFP dot plot (Fig. 2G). Taking into account that this is a multicolor FCM assay, we decided to confirm that the upper boundary for negative cells in the GFP channel was identified properly performing a fluorescence minus one (FMO) control (45). Therefore, to reveal the maximum expected fluorescence in this channel for a mating sample only when GFP fluorescence is omitted, we performed

mating reactions between stained *MAT*a and *MAT*α cells that synthesized the same GFP fragment. Consequently, although cytoplasm mixing took place no BiFC was possible and fused mating pairs remained GFP$^-$. Thus, in this cross, all mating pairs were expected to be ConA-Tet$^+$/ConA-647$^+$/GFP$^-$. The associated fluorescence seen in the GFP channel for the FMO control was similar to the fluorescence determined for stained haploid cells, confirming that an unstained haploid sample is a control that reliably identifies GFP$^+$ and GFP$^-$ events for quantitation of cell–cell fusion in fully stained samples (Supporting Information Fig. S3). In addition, the analysis of both FMO (GFP$^-$/ConA-Tet$^+$/ConA-647$^+$) and fully stained mating samples (GFP$^+$/ConA-Tet$^+$/ConA-647$^+$) in a ConA-Tet versus ConA-647 dot plot shows that mating pair subpopulation identification is correct and not affected by GFP fluorescence (Supporting Information Fig. S3), in agreement with the results obtained with *ste*2Δ × *ste*3Δ mating samples.

Compensation Controls

To verify whether the used compensation controls were the proper ones for this cell fusion analysis, we included in the standard fusion assay experiment "single-stained mating samples" obtained from wt × wt mating crosses of strains harboring the same GFP fragment where only one population
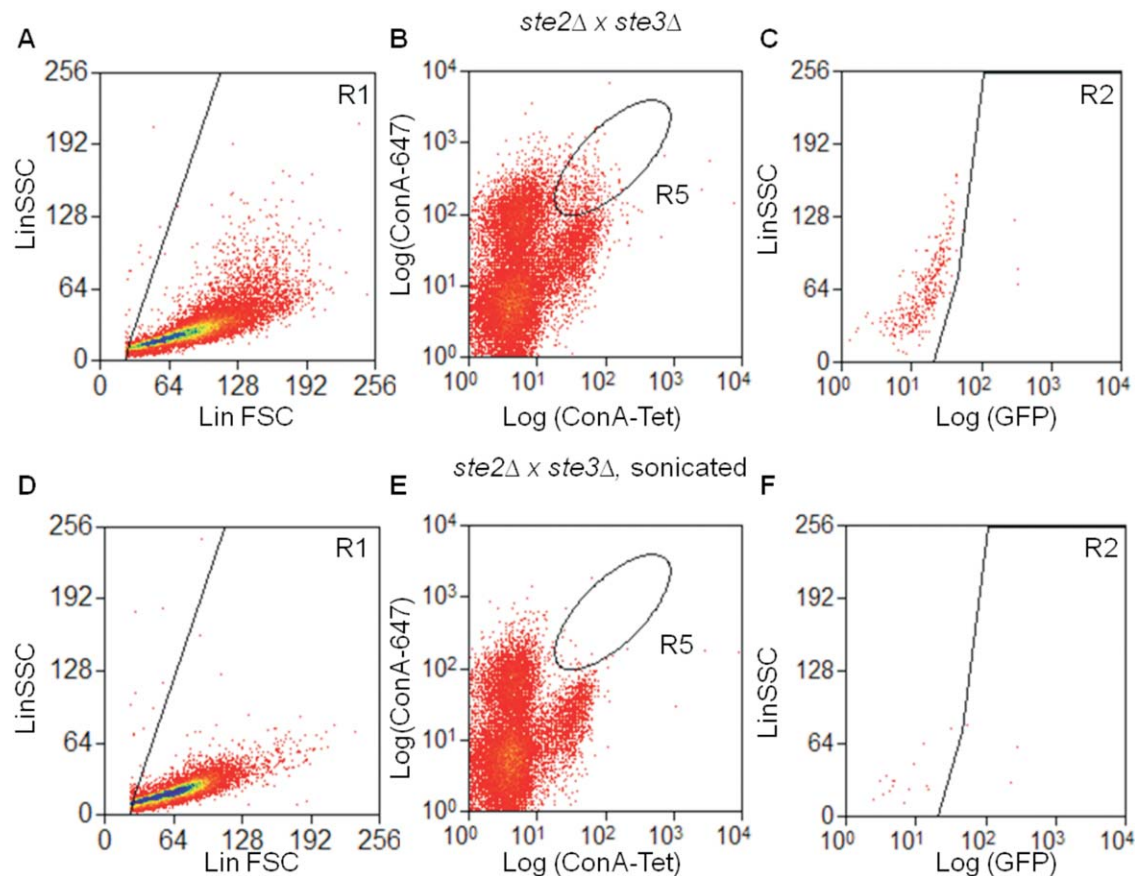
Figure 5. Mating pair subpopulation is properly gated in the mating mixture. *MAT*a *ste2Δ* × *MAT*α *ste3Δ* cross was performed under standard conditions and analyzed by FCM; representative plots are shown (**A**–**C**). R5 comprises 0.5% of total events (R1) and all of them are GFP$^-$, suggesting that they consist of cell aggregates. Consistently, these clumps were broken when samples were sonicated (**D**–**F**). [Color figure can be viewed in the online issue which is available at wileyonlinelibrary.com]

was stained. Cell fusion efficiency quantitation of wt × wt matings using single-stained haploid samples or "single-stained mating samples" as compensation controls were very similar with smaller differences than the RSE (Supporting Information Fig. S4). Thus, we conclude that haploid single-stained samples are suitable controls for compensation parameters set up, enabling a complete analysis of a mating mixture with only two strains.

Quantitation of Cell–Cell Fusion Using the Multicolor FCM Assay and Fluorescence Microscopy

To evaluate the performance of multicolor FCM assay as a method to quantify cell fusion efficiency, mating mixtures were analyzed by performing standard experiments. To this end, two haploid cell populations of *MAT*α and *MAT*a cells were stained using ConA-Tet and ConA-647, respectively. Then, mating was promoted by mixing an equal number of cells of each type allowing them to mate and fuse for more than 2.5 h at 30°C. At this point, zygotes produced are abundant but most are still freshly formed, having just either fused or begun to grow their first diploid bud (31). To analyze FCM recorded data, a standard FSC versus SSC cell gate was applied to remove debris (Fig. 6A). Then, mating pairs were identified

as double-stained entities in a ConA-647 versus ConA-Tet plot and fused and unfused subpopulations were defined by sequential gating on a SSC versus GFP dot plot. Figure 6B shows the analysis of a wt × wt mating sample. To test robustness of the multicolor FCM assay, we quantified cell fusion efficiency of a strain defective in this process as well (Fig. 6C). For this purpose, *MAT*a and *MAT*α deletion mutants of the *PRM1* gene were constructed (Supporting Information Table S1). It has been reported that if both cells of the mating pair lack this multipass plasma membrane protein, less than half of the mating pairs successfully fuse (31,32). As expected, fluorescence microscopy analysis shows that cells carrying the *prm1Δ* mutation exhibited lower fusion efficiencies than wt cells (Fig. 6D, left columns). Multicolor FCM analysis of the same mating reactions also reports this difference (Fig. 6D, right columns). A two-way analysis of variance (ANOVA, factors: method and strain) indicated that the method effect accounts for <0.1% of the total variance ($F = 0.05$, $P = 0.826$). In contrast, the strain effect accounts for 98.31% of the total variance ($F = 591.23$, $P < 0.0001$). The Bonferroni test, used here for post hoc testing of reported differences between strains, indicates that cell fusion efficiencies of wt and *prm1Δ* bilateral matings differ significantly ($P < 0.001$) in
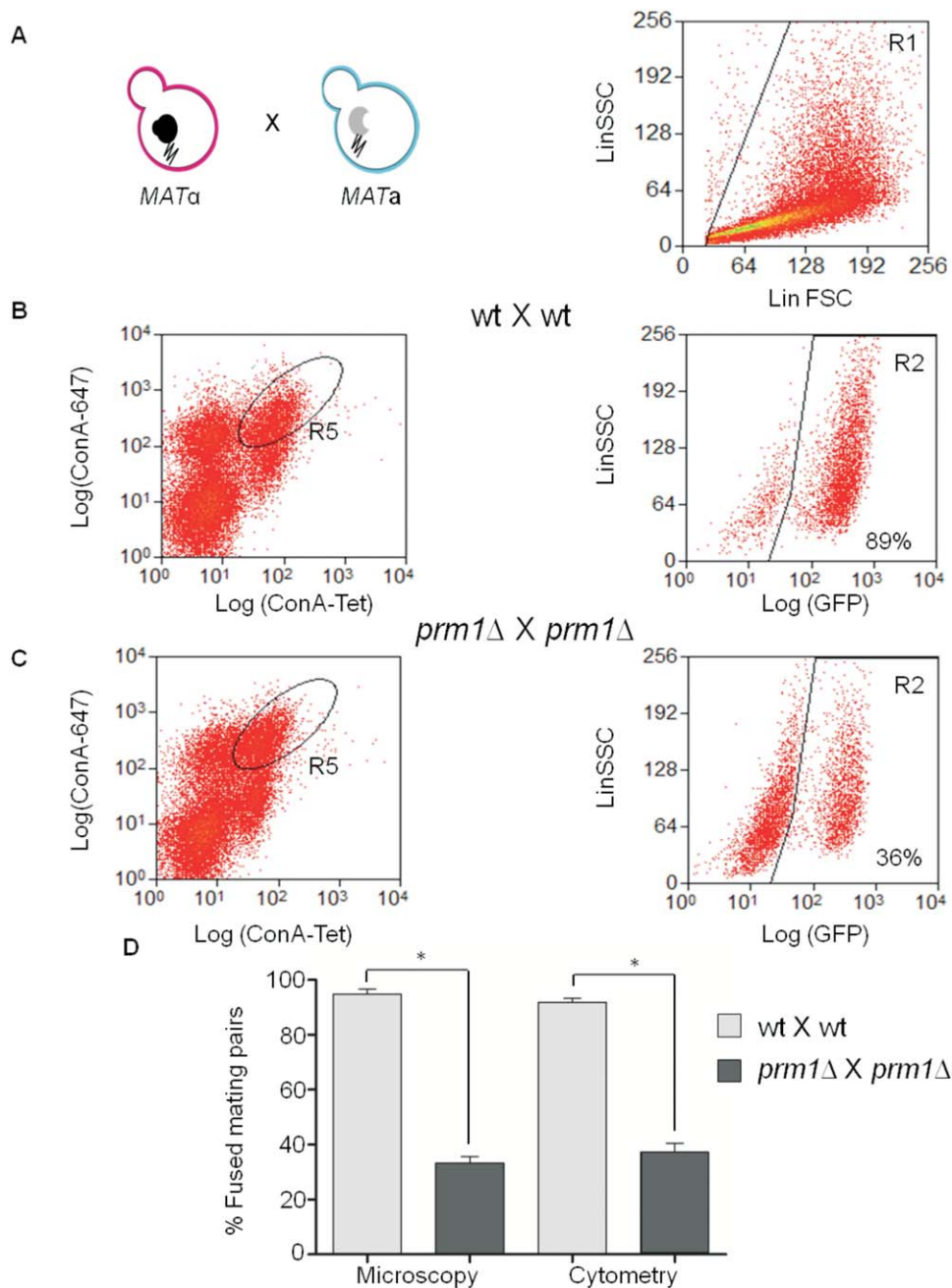
Figure 6. Multicolor FCM method to quantify cell fusion in yeast. **A**: Typical analysis of a yeast mating sample (YM2901 × YM2903). R1 was applied to all subsequent plots so that only gated events were shown, excluding cellular debris for the analysis. In all, 30,000 R1-gated events were scored per sample. **B**: Mating efficiency quantitation of a wt mating cross. Mating pair subpopulation was selected (R5) in a ConA-647 versus ConA-Tet plot. Applying R5 to a SSC versus GFP plot fused (R2) and unfused pairs were discriminated. A typical sample is shown. The percentages of gated population are shown for gate R2. **C**: Mating efficiency quantitation of a bilateral *prm1Δ* mating cross (PSAY993 × PSAY995). A typical sample is shown. The percentages of gated population are shown for gate R2. **D**: Mating efficiency quantitation of wt and a bilateral *prm1Δ* mating crosses by FCM and fluorescence microcopy. On average, 6,600 mating pairs were scored by FCM and 200 by microscopy in each sample; three mating samples were analyzed per experiment. Bars indicate mean ± SD for three independent experiments. Both methods effectively differentiate wt from mutant mating samples (*$P < 0.001$, Bonferroni test). [Color figure can be viewed in the online issue which is available at wileyonlinelibrary.com]

both methods. These results demonstrate that the multicolor FCM assay assesses yeast cell–cell fusion conserving a similar dynamic range between wild-type and cell–cell fusion defective mutants.

Typical cell fusion experiments often involve comparing several different mutants. Thus, sample-to-sample consistency is essential for accurate interpretation of the data. When we assessed the reproducibility of this novel cell fusion assay, we

found that FCM data variance did not differ significantly from microscopy variance (Levene test, $P = 0.31$). Taking altogether, these experiments demonstrate that the performance of the multicolor FCM-based assay is indistinguishable from the gold standard fluorescence microscopy-based method exhibiting high degree of reproducibility and accuracy in cell fusion efficiency determination.

DISCUSSION

We developed a novel method that uses multicolor FCM to quantify cell fusion efficiency. This method is highly reliable, fast, and robust overcoming some limitations of the widely used fluorescence microscopy-based approach. First, FCM allows the analysis of a population of mating pairs more than one order of magnitude bigger than the gold standard method. Second, observation of mating pairs either directly under the microscope or throughout registered images is subjected to different observer errors. Selection bias can favor the inclusion of morphologically normal mating pairs in the detriment of abnormal ones, regardless of whether they are fused or not. In contrast, our multicolor FCM method selects mating pairs by simple double-colored criteria defined by single-colored controls. Although we assume that approximately 2.3% of mating pairs are false, we consider this as a systematic error that it is below the interexperimental error and therefore is not relevant for final quantitation purposes. Unless automatic image analysis is employed, observation of mating pairs GFP content is also subjected to the observer bias. Based on the FMO controls, our method defines a precise threshold to quantify GFP content and therefore automatically discriminates between fused and unfused mating pairs.

Finally, the multicolor FCM method is able to register up to 3,000 mating pairs in <3 min. In comparison, a trained experimentalist invests 15 min to score 200 mating pairs using the fluorescence microscopy approach. This 75-fold decrease in sample processing is even more aggravated by eyesight extenuation associated with direct observation through a fluorescence microscope. We herein validate a new FCM-based method capable of analyzing thousands of mating pairs within minutes representing an important advance for the analysis of a large number of different mutant strains. To consider functional redundancy of fusogenic actors within or between mating partners, combinatorial analysis of candidate genes should be address. In addition, fusion efficiency in different growing conditions and treatments should be analyzed. Consequently, the high-speed quantitative analysis of cells together with its multiparameter nature makes FCM an excellent technology for high-throughput cell–cell fusion studies in yeast. Our method combines innocuous ConA–fluorophore conjugate staining of haploid cells and BiFC to define fused and unfused mating pair subpopulations in a complex mating mixture. In addition, FCM-based purification protocols of *S. cerevisiae* zygotes (46) could be adapted to obtain mating pair subpopulations by cell sorting for further analysis.

To identify and categorize genes and genetic pathways involved in cell–cell fusion, it is important to robustly quantify cell fusion efficiencies in different genetic backgrounds (e.g., single, double and multiple mutants, gene overexpression, etc.) and mating conditions. Also, it is important to phenotypically distinguish between cell fusion and other steps involved in mating such as pheromone response or mating pair formation capacities. In this regard, an alternative method described for cell–cell fusion quantitation in yeast (47) is based on the cytoplasmic mixing measuring with a β-galactosidase complementation assay in which enzyme activity is normalized to the total protein content of the sample. As many pheromone response pathway mutants decrease the total number of formed mating pairs without modifying the fused/unfused ratio, this β-galactosidase-based method is limited because a mating pair formation defect can be misread as a cell fusion defect. Yeast cell–cell fusion has also been studied using a method based on GFP BiFC and FCM (37). In this assay, a *MAT***a** strain is mixed in tenfold excess with a *MAT*α strain that produces a (red) fluorescence cytoplasmic protein. As it is assumed that the totality of the *MAT***a** cells will form a mating pair, the red fluorescence signal is used to identify the mating pairs as one-colored entities. As previously described, this method is also limited because a decrease in mating pair formation might be misinterpreted as a defect in the cell fusion as well. Therefore, in comparison to the previously reported methods, our single cell-based FCM method, like fluorescence microscopy, enables the normalization of the number of recorded fused pairs to the total number of pairs generated in the mating mixture. An additional advantage of the multicolor FCM method is that enables the quantitation of mating pair formation efficiency. Provided that durable and innocuous cell-surface labeling and BiFC can be applied, this simple method can be adapted to any other cell–cell fusion experimental models such as *C. elegans* epidermal cell fusion or mammalian fertilization (1,48).

CONCLUSIONS

In summary, we have described and validated a relatively simple method to determine yeast cell fusion efficiency providing quantitative, accurate, robust, and reproducible data necessary to accelerate advances in the identification and study of genes that might have a direct role in cell–cell fusion.

LITERATURE CITED

1. Sutovsky P. Sperm-egg adhesion and fusion in mammals. Expert Rev Mol Med 2009; 11:e11.
2. Primakoff P, Myles DG. Penetration, adhesion, and fusion in mammalian sperm-egg interaction. Science 2002;296:2183–2185.
3. Schejter ED, Baylies MK. Born to run: Creating the muscle fiber. Curr Opin Cell Biol 2010;22:566–574.
4. Pavlath GK. Spatial and functional restriction of regulatory molecules during mammalian myoblast fusion. Exp Cell Res 2010;316:3067–3072.
5. Rochlin K, Yu S, Roy S, Baylies MK. Myoblast fusion: When it takes more to make one. Dev Biol 2010;341:66–83.

6. Mi S, Lee X, Li X, Veldman GM, Finnerty H, Racie L, LaVallie E, Tang XY, Edouard P, Howes S, et al. Syncytin is a captive retroviral envelope protein involved in human placental morphogenesis. Nature 2000;403:785–789.

7. Vignery A. Macrophage fusion: Molecular mechanisms. Methods Mol Biol 2008;475:149–161.

8. Vignery A. Macrophage fusion: The making of osteoclasts and giant cells. J Exp Med 2005;202:337–340.

9. Oren-Suissa M, Hall DH, Treinin M, Shemer G, Podbilewicz B. The fusogen EFF-1 controls sculpting of mechanosensory dendrites. Science 2010;328:1285–1288.

10. Lu X, Kang Y. Cell fusion as a hidden force in tumor progression. Cancer Res 2009;69:8536–8539.

11. Ambrosi DJ, Rasmussen TP. Reprogramming mediated by stem cell fusion. J Cell Mol Med 2005;9:320–330.

12. Sapir A, Avinoam O, Podbilewicz B, Chernomordik LV. Viral and developmental cell fusion mechanisms: Conservation and divergence. Dev Cell 2008;14:11–21.

13. White JM, Delos SE, Brecher M, Schornberg K. Structures and mechanisms of viral membrane fusion proteins: Multiple variations on a common theme. Crit Rev Biochem Mol Biol 2008;43:189–219.

14. Backovic M, Jardetzky TS. Class III viral membrane fusion proteins. Curr Opin Struct Biol 2009;19:189–196.

15. Hughson FM, Reinisch KM. Structure and mechanism in membrane trafficking. Curr Opin Cell Biol 2010;22:454–460.

16. Jena BP. Membrane fusion: Role of SNAREs and calcium. Protein Pept Lett 2009;16:712–717.

17. Blond JL, Besème F, Duret L, Bouton O, Bedin F, Perron H, Mandrand B, Mallet F. Molecular characterization and placental expression of HERV-W, a new human endogenous retrovirus family. J Virol 1999;73:1175–1185.

18. Esnault C, Cornelis G, Heidmann O, Heidmann T. Differential evolutionary fate of an ancestral primate endogenous retrovirus envelope gene, the EnvV syncytin, captured for a function in placentation. PLoS Genet 2013;9:e1003400.

19. Cornelis G, Vernochet C, Carradec Q, Souquere S, Mulot B, Catzeflis F, Nilsson MA, Menzies BR, Renfree MB, Pierron G, et al. Retroviral envelope gene captures and syncytin exaptation for placentation in marsupials. Proc Natl Acad Sci USA 2015;112:E487–E496.

20. Avinoam O, Fridman K, Valansi C, Abutbul I, Zeev-Ben-Mordehai T, Maurer UE, Sapir A, Danino D, Grünewald K, White JM, et al. Conserved eukaryotic fusogens can fuse viral envelopes to cells. Science 2011;332:589–592.

21. Podbilewicz B. Virus and cell fusion mechanisms. Annu Rev Cell Dev Biol 2014;30:111–139.

22. Chen EH, Grote E, Mohler W, Vignery A. Cell-cell fusion. FEBS Lett 2007;581:2181–2193.

23. Aguilar PS, Baylies MK, Fleissner A, Helming L, Inoue N, Podbilewicz B, Wang H, Wong M. Genetic basis of cell-cell fusion mechanisms. Trends Genet 2013;29:427–437.

24. Ydenberg CA, Rose MD. Yeast mating: A model system for studying cell and nuclear fusion. Methods Mol Biol 2008;475:3–20.

25. Herskowitz I. MAP kinase pathways in yeast: for mating and more. Cell 1995;80:187–197.

26. Bardwell L. A walk-through of the yeast mating pheromone response pathway. Peptides 2005;26:339–350.

27. White JM, Rose MD. Yeast mating: Getting close to membrane merger. Curr Biol 2001;11:R16–R20.

28. McCaffrey G, Clay FJ, Kelsay K, Sprague GF Jr. Identification and regulation of a gene required for cell fusion during mating of the yeast *Saccharomyces cerevisiae*. Mol Cell Biol 1987;7:2680–2690.

29. Trueheart J, Fink GR. The yeast cell fusion protein fus1 is O-glycosylated and spans the plasma membrane. Proc Natl Acad Sci USA 1989;86:9916–9920.

30. Nolan S, Cowan AE, Koppel DE, Jin H, Grote E. Fus1 regulates the opening and expansion of fusion pores between mating yeast. Mol Biol Cell 2006;17:2439–2450.

31. Heiman MG, Walter P. Prm1p, a pheromone-regulated multispanning membrane protein, facilitates plasma membrane fusion during yeast mating. J Cell Biol 2000;151:719–730.

32. Jin H, Carlile C, Nolan S, Grote E. Prm1 prevents contact-dependent lysis of yeast mating pairs. Eukaryot Cell 2004;3:1664–1673.

33. Engel A, Aguilar PS, Walter P. The yeast cell fusion protein Prm1p requires covalent dimerization to promote membrane fusion. PLoS One 2010;5:e10593.

34. Olmo VN, Grote E. Prm1 targeting to contact sites enhances fusion during mating in *Saccharomyces cerevisiae*. Eukaryot Cell 2010;9:1538–1548.

35. Aguilar PS, Engel A, Walter P. The plasma membrane proteins prm1 and fig1 ascertain fidelity of membrane fusion during yeast mating. Mol Biol Cell 2007;18:547–556.

36. Grote E. Cell fusion assays for yeast mating pairs. Methods Mol Biol 2008;475:165–196.

37. McCullagh E, Seshan A, El-Samad H, Madhani HD. Coordinate control of gene expression noise and interchromosomal interactions in a MAP kinase pathway. Nat Cell Biol 2010;12:954–962.

38. Longtine MS, McKenzie A, Demarini DJ 3rd, et al. Additional modules for versatile and economical PCR-based gene deletion and modification in *Saccharomyces cerevisiae*. Yeast 1998;14:953–961.

39. Janke C, Magiera MM, Rathfelder N, Taxis C, Reber S, Maekawa H, Moreno-Borchart A, Doenges G, Schwob E, Schiebel E, et al. A versatile toolbox for PCR-based tagging of yeast genes: New fluorescent proteins, more markers and promoter substitution cassettes. Yeast 2004;21:947–962.

40. Tkacz JS, Cybulska EB, Lampen JO. Specific staining of wall mannan in yeast cells with fluorescein-conjugated concanavalin A. J Bacteriol 1971;105:1–5.

41. Porro D, Ranzi BM, Smeraldi C, Martegani E, Alberghina L. A double flow cytometric tag allows tracking of the dynamics of cell cycle progression of newborn *Saccharomyces cerevisiae* cells during balanced exponential growth. Yeast 1995;11:1157–1169.

42. Porro D, Srienc F. Tracking of individual cell cohorts in asynchronous *Saccharomyces cerevisiae* populations. Biotechnol Prog 1995;11:342–347.

43. Burkholder AC, Hartwell LH. The yeast alpha-factor receptor: Structural properties deduced from the sequence of the ste2 gene. Nucleic Acids Res 1985;13:8463–8475.

44. Hagen DC, McCaffrey G, Sprague GF Jr. Evidence the yeast ste3 gene encodes a receptor for the peptide pheromone a factor: Gene sequence and implications for the structure of the presumed receptor. Proc Natl Acad Sci USA 1986;83:1418–1422.

45. Tung JW, Heydari K, Tirouvanziam R, Sahaf B, Parks DR, Herzenberg LA, Herzenberg LA. Modern flow cytometry: A practical approach. Clin Lab Med 2007;27:453–468.

46. Zapanta Rinonos S, Saks J, Toska J, Ni CL, Tartakoff AM. Flow cytometry-based purification of *S. cerevisiae* zygotes. J Vis Exp 2012;67:4197.

47. Grote E. Secretion is required for late events in the cell-fusion pathway of mating yeast. J Cell Sci 2010;123:1902–1912.

48. Alper S, Podbilewicz B. Cell fusion in *Caenorhabditis elegans*. Methods Mol Biol 2008;475:53–74.